MANSOURA JOURNAL OF Physics
Official Journal of Faculty of Science, Mansoura University, Egypt
E-mail: scimag@mans.edu.eg ISSN: 2974-4954

Structural studies on borate compounds modified by $MgCO_3$, $ZnCO_3$, and fructose

Samar S.Khater[1], Hosam Salaheldin[2], G. El-Damrawi[3]

[(1,3)] Glass Research Group, Physics Department, Faculty of Science, Mansoura University, 35516, Egypt

[(2)]Biophysics Research Group, Physics Department, Mansoura University, Egypt

**Corresponding author: samarkhater00@gmail.com*

Received:24/7/2023
Accepted:6/9/2023

Abstract: Magnesium fructoborate of chemical formula, $Mg(C_6H_{10}O_6BO)_2 3.5H_2O$ was prepared using a chemical wet process. The fructose-containing boron organic ester is formed and modified in solution. The FTIR, NMR, and Raman spectroscopies are used to examine the distinguished borate structural units. The strong amorphous material has been produced by modification using $ZnCO_3$ or $MgCO_3$. To identify the various kinds and concentrations of borate derivatives contained in products, ^{11}B NMR solutions and Raman spectroscopy were developed. The modifier part of fructose and magnesium carbonate is consumed to change B_2O_3 from three to four coordinated borate units. The presence of the borate-boroxol ring as the primary structural component is confirmed by the Raman spectra of pure B_2O_3. But when fructose and magnesium carbonate are added, various borate units are created. $ZnCO_3$ modification has a less significant impact on boron transformation than $MgCO_3$ modification does.

keywords: Calcium fructose, ^{11}B NMR spectroscopy, Borate esters.

1. Introduction

Several plant and animal living organisms involve the element boron [1-4]. Understanding how boron works chemically in food is significant. Various reports [1–7] have described the relationship between calcium (Ca) and boron (B), which has been found in plants, microorganisms, animals, and people. However, experimental research is currently being done to determine the actual nature of the Ca/B relationship. Applications and effects of calcium carbonate and sugar fracture on the borate structural units have revealed that it shares a chemical structure with the boro-carbohydrates that naturally occur in edible plants [4–8]. Some experimental investigations have confirmed that boron is present in plants as ester groups [9,10]. Then the optimal chemical form for absorption into cells is boron sugar esters.

Previous research has demonstrated that boron as a natural complex can be simply identified [9–11]. The boric acid esters can be represented by the isolated soluble complexes from a few particular plant species. For a very long time, boron supplements have included boric acid and various inorganic borates [4–9].

In the pharmaceutical industry, calcium fructoborate (CFB) has recently been demonstrated to have interesting antioxidant effects in addition to cancer actions [8-12]. In addition, CFB can serve as an unappreciated role in preventing males from acquiring prostate cancer. This is because boric acid prevents some human prostate cancer cells from proliferating. In addition, CFB can work cooperatively to maintain strong and sturdy vertebrae of bone [7-13].

The primary purpose was to specify boron distribution in free and chelated forms by analyzing the major structure. of borate units modified by $CaCO_3$, $MgCO_3$, and $ZnCO_3$. The most interest of such a study is to find out the specific relation between the N_4 fraction given by NMR spectroscopy and BO_3, BO_4 units as essential derivatives free H_3BO_3.

2. Methodology

2.1 Sample preparation

D-fructose (2.16 g) with purity (≥98%) was dissolved in 4 ml of distilled water, followed by 0.372 g of H_3BO_3 with purity (99%) and 0.246 g of $MgCO_3$ with purity (40%). 20 ml of

acetone was added after the whole evolution of carbon dioxide from the reaction, resulting in the formation of colorless oil at the bottom of the conical flask, separated using a separation funnel. The resultant product was triturated with a glass rod to stimulate crystallization, resulting in the creation of a white, crystalline solid material that was washed again with acetone. The solvent was allowed to evaporate at room temperature, yielding pure Mg-fructoborate with a 0.78% yield. The same technique was followed to create Zn-Mg-Fructoborate.

2.2 Measurements

To measure X-ray diffraction, a Shimadzu X-ray diffractometer is employed (the apparatus type Dx-30, Metallurgy Institute, El Tebbin, Cairo, Egypt).

The powdered samples' NMR spectra were captured using a Joel NMR 500 (11.74T, Mansoura University) spectrometer. To solve the issue of the relaxation time, one pulse detection technique was used. Pulses with a duration of 2-3 s, an angle of around 45^{o}, and substantial delays (25 s) between them were gathered. Up to 1400 scans were accumulated depending on the specific sample.

Raman spectra were collected using a Jobin Yvon—HR640 spectrometer with an Andor CCD detector (DU420A-BR-DD model). During the experiment, a 532 nm laser source with an average power of 63.02 mW was used. The spectra were taken at room temperature with a 10-minute exposure duration.

3. Results and Discussion

3.1 XRD spectroscopy

The XRD spectra of H_3BO_3 modified by $ZnCO_3$ and $MgCO_3$ are displayed in Figure 1. The formation of multiple borate units leads the system to become amorphous and prevents crystallization from taking place. According to the XRD patterns shown in Figure 1, the studied magnesium fructoborate network contains a non-order structure species involving ring [$BO_{3/2}$] units as the predominant forming species. Additionally, B_2O_3, which is made from H_3BO_3, has the highest tendency for forming a glassy network even at extremely high modifier content. This characteristic has given rise to the hypothesis that B_2O_3 material exhibits abnormal characteristics, sometimes known as a crystallization anomaly for boron oxide [14,15].

There are three broad diffraction patterns in the XRD spectra of the borate matrix containing $ZnCO_3$ (pattern b). They can be assigned to the presence of two separated glass former species, which are B_2O_3 and a portion from $ZnCO_3$. In all cases, it could be considered that B_2O_3 never crystallizes under ambient conditions.

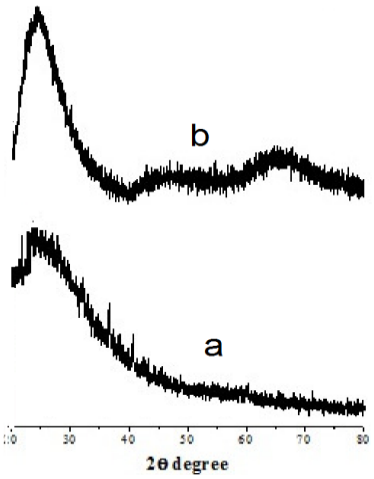

Figure 1. X-ray diffraction pattern of fluoro-borate containing (a) $MgCO_3$ (b) $ZnCO_3$.

On the other hand, when B_2O_3 has a significant quantitative value of BO_3, which may disperse in a chain-like shape [4,12], B_2O_3 can crystallize easily. In this instance, the vitreous B_2O_3 matrix is made up of insights of B_3O_9 rings, which are made up of [$BO_{3/2}$] units, some of which are attached to tetrahedral boron atoms.

3.2 Raman spectroscopy

The Raman band resolution for pure H_3BO_3 or B_2O_3 at about 876 cm^{-1}, as depicted in Figure 2a can be confirmed by the previously mentioned consideration based on XRD pattern results. There is just one resolved peak in the Raman spectra (Figure 2a), which indicates that the boroxol ring was dominantly formed and represented by the sharp Raman peak around 876 cm^{-1}. When H_3BO_3 is modified by both $MgCO_3$ and $ZnCO_3$ molecules, the well-formed species are non-ring (chain BO_3), planner BO_3, and BO_4 groups, as illustrated in Figure 2 (b and c). The change of the B_3O_9 ring to both planner BO_3 and BO_4 is clarified by the forming of the well-resolved spectrum at about 1100 cm^{-1}.

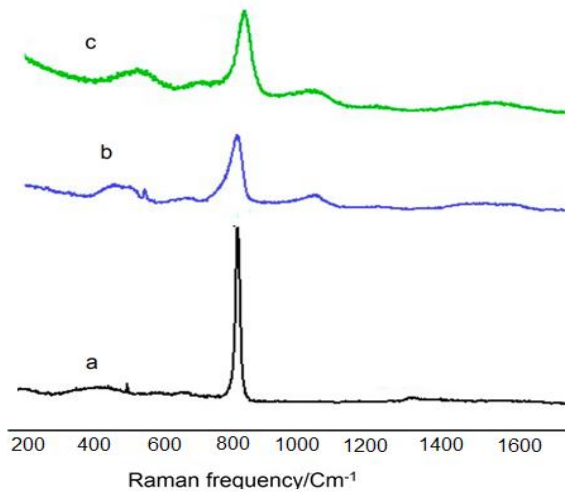

Figure 2. Measured spectra for (a) pure borate matrix modified by (b) $MgCO_3$ and (c) $ZnCO_3$.

The insertion of a modifier to the B_2O_3 or H_3BO_3 network then causes various changes. H_3BO_3 molecules can be converted to B_2O_3 and H_2O molecules. $MgCO_3$ or $ZnCO_3$ modifiers can be converted to MgO, ZnO, and CO_2. Then, as a previous species, both OH and CO_2 groups can link with B_2O_3, creating mono or di-ester groups. Furthermore, boron-oxygen-boron (B-O-B) bonds can be disrupted by oxygen anions produced by the modifier (Mg++ / -O-B). High concentrations of the modifier can create a (BO_4) with (3BO) and (1NBO) ions. Then the process of modification varies between different types of glass systems. When comparing the B_2O_3 structure to that of the phosphate and silicate networks, the reverse modifications are taken into account. Additionally, the B_2O_3 is made up of trigonal ($BO_{3/2}$) groups, as a direct result of the addition of a modifier, the charged [B_4]-tetrahedral units The different modifications included in the borate matrix result in several unusual behaviors in the B_2O_3 network. This attracted attention derives mostly from the B_2O_3 matrix's unusual behavior in forming different types of borate units. The latter are well-defined configurations of the fundamental BO_3 and BO4 structures. The main approaches for determining the quantity of BO_3 and BO_4 are NMR and Raman spectroscopy [16,17]. The greatest N_4 percentage has been demonstrated to be between 33 and 40 mol% modifier oxide, with a ratio of around 0.45 BO_4 to 0.55 BO_3.

3.3 ^{11}B NMR spectroscopy

The coupled behavior of (B) and (O) involves positive and negative components that cancel each other out, which is why a singlet is visible in the ^{11}B NMR spectra of H_3BO_3, Figure 3.

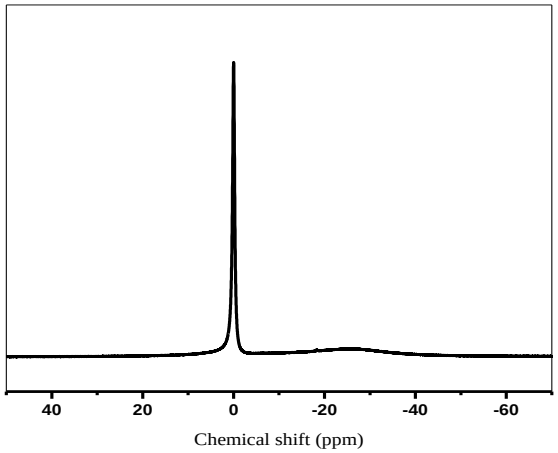

Figure 3. ^{11}B NMR spectra of boron nuclei in H_3BO_3

However, the interaction between B and O in the $CaCO_3$ or $MgCO_3$ fructoborate units (CaFB or MgFB) differ greatly and cannot be canceled out, leading to the observation of several resonance lines in the ^{11}B NMR spectra of both $MgCO_3$ and CaFB. However, the relation between the boron and oxygen in the modified $CaCO_3$ or $MgCO_3$ fructoborate units (CaFB or MgFB) differs significantly and cannot be eliminated, which led to the detection of multiple resonance lines in the ^{11}B NMR spectra of both MgCO3 and CaFB, Figures 4 and 5.

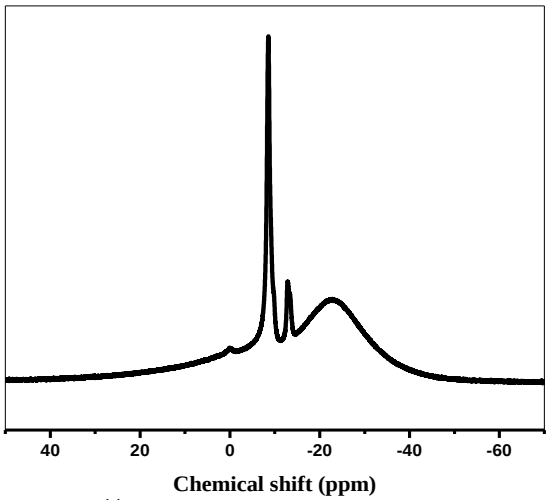

Figure 4. ^{11}B NMR spectra of a boron atom in MgFB compounds.

The preceding graphs demonstrate how the experimental spectra of H_3BO_3 (at 0 ppm) lack the sharp resonance peak at 0 ppm. These findings lead to the conclusion that the conversion of free H_3BO_3 (0 ppm) into further

derivatives, such as BO_3, BOC_2, BOH, and BO_4 units, was enhanced by both fructose and magnesium carbonate, acting as modifier species. The NMR resonance envelope at about -8.5 ppm, -12.8 ppm, and another at -22.5 ppm support these hypotheses. As shown in Figure 6, the change in tetrahedral boron proportion as $ZnCO_3$ is increased at the expense of $MgCO_3$. According to Figure 6, N_4 is highest at 0 $ZnCO_3$ and subsequently falls as $ZnCO_3$ rises.

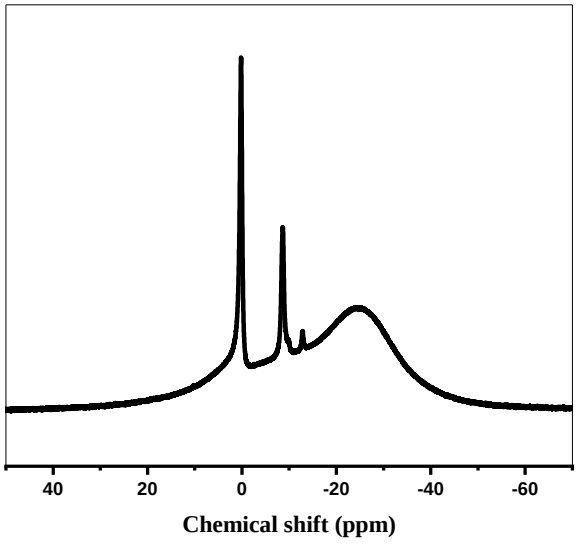

Figure 5. ^{11}B NMR resonance of a boron atom in ZnFB compounds

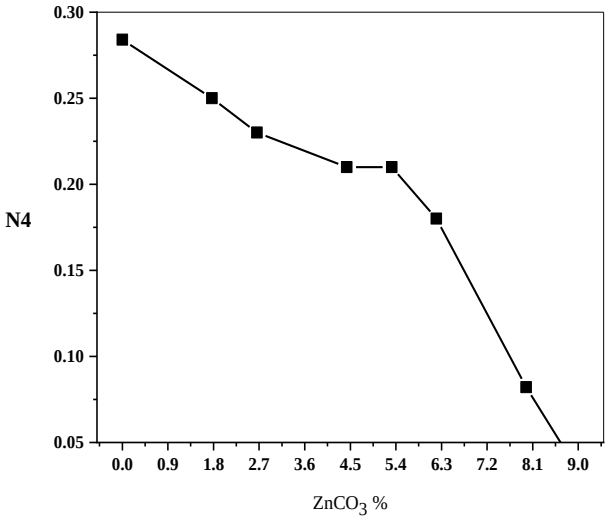

Figure 6. The relation between the change of N_4 and the increase of $ZnCO_3$ at the expense of $MgCO_3$

4. Conclusion

The well-obtained borate composition is studied using XRD spectroscopy. Upon modification with $ZnCO_3$ or $MgCO_3$, the fluoroborate compound's amorphous form plays an enormous role. To determine the different types and concentrations of borate derivatives present in products, ^{11}B NMR and Raman spectroscopy were created. Due to changes caused by $MgCO_3$ molecules, the four coordinated units can be formed. Raman spectrum of pure B_2O_3 shows that the borax-borate ring exists as the primary structural component. Magnesium carbonate and fructose can modify borate units to produce various borate units. A few changes were made to the boron transformation by $ZnCO_3$. The production of mono-, di-, and triester groups as bio-derivative unit derivative esters has been confirmed by NMR spectra of boron, proton, and carbon nuclei.

5. References

1 Mavi B., I. Akkurt, (2010) Natural radioactivity, and radiation hazards in some building materials used in Isparta, Turkey, Radiation Physics and Chemistry, **79,** 933-937.

2 Fan E., L. Zhang, S. Jiang, Y. Bai, (2008) Beneficial effects of resveratrol on atherosclerosis, *Journal of medicinal food*, **11,** 610-614.

3 Packard R.R., P. Libby, (2008) Inflammation in atherosclerosis: from vascular biology to biomarker discovery and risk prediction, Clinical chemistry, **54,** 24-38.

4 Militaru C., I. Donoiu, A. Craciun, I.D. Scorei, A.M. Bulearca, R.I. Scorei, (2013) Oral resveratrol and calcium fructoborate supplementation in subjects with stable angina pectoris: effects on lipid profiles, inflammation markers, and quality of life. *Nutrition*, **29,** 178-183.

5 Nielsen F.H., C.D. Hunt, L.M. Mullen, J.R. Hunt, (1987) Effect of dietary boron on mineral, estrogen, and testosterone metabolism in postmenopausal women 1, *The FASEB journal*, **1,** 394-397.

6 Rondanelli M., M.A. Faliva, G. Peroni, V. Infantino, C. Gasparri, G. Iannello, S. Perna, A. Riva, G. Petrangolini, A. Tartara, (2020) Pivotal role of boron supplementation on bone health: A narrative review, *Journal of Trace Elements in Medicine and Biology*, **62** 126577.

7 Allen B.C., P.L. Strong, C.J. Price, S.A. Hubbard, G.P(1996). Daston, Benchmark

dose analysis of developmental toxicity in rats exposed to boric acid, Fundamental and Applied Toxicology, **32** 194-204.

8 Marone P.A., J.T. Heimbach, B. Nemzer, J.M. Hunter, (2016) Subchronic and genetic safety evaluation of a calcium fructoborate in rats, Food and Chemical Toxicology, **95** 75-88.

9 Singh A.K., N. Kewalramani, V. Mani, A. Sharma, P. Kumari, R.P. Pal, (2021) Effects of boric acid supplementation on bone health in crossbred calves under tropical condition, *Journal of Trace Elements in Medicine and Biology*, **63** 126647.

10 Bashir N.Z., M. Krstic, (2021). Boric acid as an adjunct to periodontal therapy, DOI: 10.1111/idh.12487.

11 Scorei R., P. Rotaru, (2011) Calcium fructoborate: potential antiinflammatory agent. *(published online ahead of print January* 28, , *Bio Trace Elem Res doi*, **10**.

12 Miljkovic D., R.I. Scorei, V.M. Cimpoiaşu, I.D. Scorei, (2009). Calcium fructoborate: plant-based dietary boron for human nutrition, *Journal of dietary supplements*, **6,** 211-226.

13 Sevim F., F. Demir, M. Bilen, H. Okur, (2006). Kinetic analysis of thermal decomposition of boric acid from thermogravimetric data, *Korean Journal of Chemical Engineering*, **23,** 736-740.

W. The crystal structure of cubic metaboric acid, Acta Crystallographica, **16,** 380-384.

15 Huber C., S. Setoodeh Jahromy, C. Jordan, M. Schreiner, M. Harasek, A. Werner, F. Winter, (2019) Boric acid: a high potential candidate for thermochemical energy storage. Energies, **12,** 1086.

16 El Bouraie M.M., S.S. Ibrahim (2021), Comparative study between metronidazole residues disposal by using adsorption and photodegradation processes onto MgO nanoparticles, *Journal of Inorganic and Organometallic Polymers and Materials*, **31** 344-364.

17 El Baz N., G. El-Damrawi, A.M. Abdelghany, (2021) Structural Role of CeO2 in the Modified Borate Glass-Ceramics. *New Journal of Glass and Ceramics*, **11** 34-43.

18 Yano T., N. Kunimine, S. Shibata, M. Yamane, (2003) Structural investigation of sodium borate glasses and melts by Raman spectroscopy. II. Conversion between BO4 and BO2O− units at high temperature, *Journal of Non-Crystalline Solids*, **321** 147-156.

19 Kapoor S., H.B. George, A. Betzen, M. Affatigato, S. Feller, (2000) Physical properties of barium borate glasses determined over a wide range of compositions, *Journal of non-crystalline solids*, **270** 215-222.

20 Gilboy M.B., S. Heinerichs, G. Pazzaglia (2015), Enhancing student engagement using the flipped classroom, *Journal of nutrition education and behavior*, **47** 109-114.